Generation of ultrahigh harmonics with a two-stage free electron laser and a seed laser

V. V. Goloviznin* and P. W. van Amersfoort
FOM Institute for Plasma Physics ''Rijnhuizen,'' P.O. Box 1207, 3430 BE Nieuwegein, The Netherlands
(Received 23 October 1995)

We consider the possibility to premodulate an ultrarelativistic electron beam on the nanometer length scale, so that it can produce coherent spontaneous radiation in the x-ray range. The scheme that uses the same basic elements as the high gain harmonic generation (HGHG) scheme, two wigglers and a conventional seed laser, is shown to suit this task if the process of premodulation occurs at zero net gain of the seed-laser wave. Operation with zero gain provides the opportunity to reach much higher harmonics than in the original HGHG technique. The output radiation is tunable between discrete harmonics of the seed frequency. The total length of the periodic magnetic structure is shown to be of the order of several meters, an order of magnitude shorter than that required for self-amplified spontaneous emission (SASE). For a beam quality similar to that in the SASE scheme and with realistic seed-laser parameters, the efficiency of the beam premodulation at the 50th harmonic (5 nm for a seed wavelength of 250 nm) is shown to be as high as 15%. [S1063-651X(97)16805-2]

PACS number(s): 41.60.Cr

I. INTRODUCTION

One of the most challenging problems in modern free electron laser (FEL) technology is to operate in the x-ray region, especially in the ''water window.'' Because of the absence of suitable optical resonators in this range of wavelengths, only a single-pass device may suit this task. The self-amplified spontaneous emission (SASE) mechanism [1] has been proposed as a way to provide high-power coherent emission in the x-ray range. At present, both the undulator parameters and the electron-beam parameters that are required for lasing are believed to be achievable. The SASE approach should be noted, however, to rely on the establishment of a coherent mode from incoherent noise, a process that is not yet well understood in a single-pass device. In addition, SASE implies working with a very long magnetic structure, typically several tens of meters long [2]. This is mainly because of the rather long build-up time necessary to establish the coherent mode.

The situation would be very much improved if a short-period premodulation of the electron-beam density were possible with an external source. This premodulation can be transformed by an FEL into a coherent electromagnetic wave, and if the spatial period of the premodulation is sufficiently small, coherent x-ray radiation will be produced. The high-gain harmonic generation (HGHG) scheme has been proposed in [3] as a possible way to create a premodulation of the electron beam at a high spatial frequency (see the schematic layout in Fig. 1). Namely, an FEL amplifier, operating in the high-gain regime, has been shown to produce a considerable beam density modulation (as well as a certain amount of coherent radiation) at the third harmonic of the fundamental frequency. With the help of an additional single-pass FEL operating at a frequency which is three times higher than that of the first FEL, this seed modulation may be transformed into short-wavelength radiation and amplified up to saturation [4]. As the coherent input signal for the first amplifier is not available below ~ 160 nm, the HGHG technique enables expansion of the range of FEL operation down to 50 nm, at best. For shorter wavelengths, another approach is necessary.

In the present paper we consider a scheme that uses the same basic elements as the HGHG scheme (see Fig. 1), two wigglers and a conventional seed laser. The main difference with the HGHG technique is that in our scheme the process of premodulation occurs at zero net gain of the seed wave. This provides the opportunity to reach much higher harmonics than in the HGHG approach. Numerical simulations are made and estimates are given for the efficiency of the premodulation, the output radiation power and the total length of the periodic magnetic structure.

The paper is organized as follows. In Sec. II we consider the design of the first stage of the device and study the conditions necessary for efficient beam premodulation. Coherent x-ray emission with the premodulated beam is considered in Sec. III. Section IV contains the results of numerical simulations.

II. BUNCHING

The first part of the two-stage FEL, the buncher, is a wiggler that provides interaction between the seed laser and the

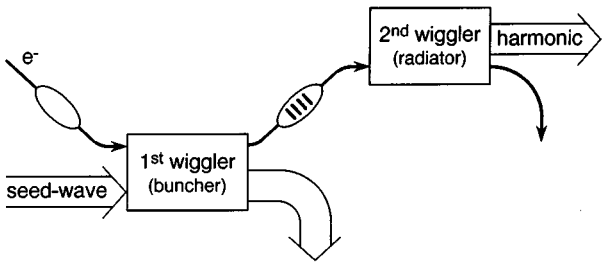

FIG. 1. Schematic layout of the harmonic generation technique that involves beam premodulation and the subsequent coherent photon production.

*Permanent address: Russian Research Center Kurchatov Institute, 123182 Moscow, Russia.

electron beam. We assume the first wiggler to be a helical one to provide the most efficient laser-particle interaction. As we will see, an optimal design implies a high first wiggler parameter, up to $a_{w1}\sim 4-5$, in order to reduce the length of this wiggler and to decrease the influence of the angular spread in the beam.

We adopt a simplified one-dimensional (1D) approach for the description of both electron beam and electromagnetic radiation; possible 3D effects are not addressed. The validity of this approximation is discussed in Sec. IV. In 1D approximation, the motion of an ultrarelativistic electron in the combined field of a circularly polarized laser wave and a helical wiggler is described with the well-known set of equations [5] (note the usage of relativistic units $\hbar=c=1$ throughout this paper)

$$\frac{d\epsilon}{dz}=\frac{m^2\omega_0}{\epsilon}\,a_{w1}a_s\sin\Phi, \tag{1}$$

$$\frac{d\Phi}{dz}=\omega_0\left(\frac{1}{v_z}-1\right)-\Omega_{w1}, \tag{2}$$

where m is the electron mass, z is the particle coordinate along the wiggler axis, $\Phi\equiv\omega_0 t-(\omega_0+\Omega_{w1})z$ is the particle phase with respect to the ponderomotive potential well, ϵ and v_z are the particle energy and longitudinal velocity, ω_0 and $a_s=eE_0/m\omega_0$ are the frequency of the laser wave and its normalized intensity, and $\Omega_{w1}=2\pi/\lambda_{w1}$ is the spatial wiggler frequency. The above equations are often referred to as the ''pendulum equations'' because of the similarity between Eqs. (1) and (2) and the equations of motion of a massive point in an external coslike potential well. The initial conditions for Eqs. (1) and (2) correspond to a nonmodulated beam at the entrance of the wiggler: $\Phi(z=0)$ is assumed to be uniformly distributed from 0 to 2π. The results obtained with the above set of equations must be averaged over the initial electron energy spread and the initial angular spread in the electron beam.

The basic idea of how to transform the seed frequency into a very high harmonic consists in the simple observation that in a parabolic potential well all particles having started their motion at zero initial velocity meet each other in the center of the well after exactly a quarter of an oscillation period. In other words, the initial spatially uniform particle distribution is transformed into a δ-like distribution that formally has nonvanishing amplitudes of infinitely high Fourier components. The coslike ponderomotive potential appearing in Eqs. (1) and (2) is similar, in a sense, to a periodic sequence of parabolic wells. One may thus expect that after a certain distance in the wiggler the particle distribution over the longitudinal coordinate is periodically modulated in such a way that the spatial period coincides with the seed-laser wavelength but the Fourier transformation contains very high harmonics. As a result, the electron bunch splits into thin current sheets orthogonal to the bunch axis. Upon injection into a short-period undulator, such a current sheet emits coherently if the radiated electromagnetic wave (as determined by the undulator parameters) has a wavelength longer than the sheet thickness.

The δ-like distribution is, of course, never reached in reality. In 1D approach, there are two main factors limiting width of a current sheet. First, the initial energy spread and angular spread in the electron beam lead to a nonzero initial velocity of an electron with respect to the ponderomotive potential well. Second, the potential well itself is anharmonic, therefore the oscillation period depends on the amplitude of oscillation, and different particles reach the center of the well at different instants of time. In addition, the current sheets are dynamical objects, therefore their thickness is time dependent. All the above factors should be taken into account when considering the efficiency of x-ray generation.

It is convenient to switch from ϵ and z to new dimensionless variables u and τ such that

$$u=\frac{\epsilon^2}{\langle\epsilon^2\rangle}-1 \tag{3}$$

and

$$\tau=\frac{\omega_0 z m^2}{\langle\epsilon^2\rangle}\sqrt{a_s a_{w1}(1+a_{w1}^2)}, \tag{4}$$

where $\langle\epsilon^2\rangle$ is the mean-squared particle energy in the beam and u is assumed to be small, $|u|\ll 1$. Expanding Eqs. (1) and (2) to the first order in u, combining them and averaging over one wiggler period, one obtains the second-order differential equation

$$\ddot{\Phi}=-\sin\Phi \tag{5}$$

with the initial condition

$$\dot{\Phi}(\tau=0)=\frac{1}{2}\left(\frac{1+a_{w1}^2}{a_s a_{w1}}\right)^{1/2}\left(1-\frac{2\langle\epsilon^2\rangle\Omega_{w1}}{m^2\omega_0(1+a_{w1}^2)}+\frac{\langle\epsilon^2\rangle v_\perp^2}{m^2(1+a_{w1}^2)}-u_0\right), \tag{6}$$

where $u_0\equiv u(\tau=0)$ and an overdot refers to the derivative $d/d\tau$. Equation (5) contains no input parameters and describes small-amplitude oscillations with a period of 2π (for $|\Phi|\ll 1$). In dimensional variables, the length of the first wiggler that provides the best bunching is therefore

$$L_{w1}\sim\frac{\pi}{2}\,\frac{\langle\epsilon^2\rangle}{\omega_0 m^2[a_s a_{w1}(1+a_{w1}^2)]^{1/2}}. \tag{7}$$

From Eq. (7) one can see the advantage of a high a_{w1}: the length of the buncher may be reduced considerably as compared to the case $a_{w1}\sim 1$.

As was already mentioned, efficient particle premodulation requires a small initial ''velocity'' $\dot{\Phi}(\tau=0)$. One sees from Eq. (6) that the condition

$$\langle\epsilon^2\rangle=m^2(1+a_{w1}^2)\left(\frac{2\Omega_{w1}}{\omega_0}-\langle v_\perp^2\rangle\right)^{-1} \tag{8}$$

provides $\langle\dot{\Phi}(\tau=0)\rangle=0$ where $\langle\ \rangle$ means averaging over the beam. Equation (8) may be considered as a resonance condition relating the beam energy to the parameters of the first wiggler and the seed laser. The above condition is distinctly different from that of the HGHG approach. Namely, amplification of an electromagnetic wave in an FEL is known to

originate from overall deceleration of an electron beam; therefore, the gain curve reaches its maximum at a beam velocity that is slightly above the phase velocity of the ponderomotive potential well responsible for the interaction between the beam and the electromagnetic wave. The HGHG scheme operates at a maximum of gain, while Eq. (8) corresponds to exact resonance between the electron beam and the ponderomotive potential, and, respectively, to zero net gain of the laser wave.

If the above condition is satisfied, the remaining spread in $\dot{\Phi}(\tau=0)$ is due to individual deviations of the electron initial energy and the transverse velocity from the averaged values. From Eq. (6) one may see another advantage of having a high a_{w1}: the term describing the transverse velocity contribution is suppressed in this case with a large factor $(1+a_{w1}^2)^{-1}$. The influence of the angular spread, as compared to that of the energy spread, is seen to be negligible if the following inequality holds:

$$\langle v_\perp^2 \rangle < \frac{m^2(1+a_{w1}^2)\sigma}{\langle \epsilon^2 \rangle}, \tag{9}$$

where σ is the relative energy spread in the electron beam. In the further considerations we will assume this condition to be valid.

A simple estimate can be made concerning the influence of the initial energy spread on the bunching efficiency. During a time τ, a small initial ''velocity'' $\dot{\Phi}(\tau=0)$ would result in an additional phase shift $\Delta\Phi \sim \tau\dot{\Phi}(\tau=0)$. To provide coherent emission at the nth harmonic of the seed frequency, one should keep $\Delta\Phi < \pi/n$ at the time $\tau \sim \pi/2$. A typical value of u_0 is $|u_0| \sim 2\sigma$. Using Eq. (6) one finds the condition

$$\frac{\sigma}{2}\left(\frac{1+a_{w1}^2}{a_s a_{w1}}\right)^{1/2} < \frac{1}{n}. \tag{10}$$

Hence, to reach the highest frequency up-conversion, the best beam quality (small σ) and the highest seed-laser power (large a_s) are necessary.

For further considerations, it is convenient to introduce a dimensionless parameter s,

$$s = \frac{2}{n\sigma}\left(\frac{a_s a_{w1}}{1+a_{w1}^2}\right)^{1/2}. \tag{11}$$

Simple intuitive reasoning shows that an optimal buncher design corresponds to $s \sim 1$, when the length of current sheets is about half a wavelength of the output radiation. For much lower s, the current sheets are significantly thicker; therefore, the Fourier component of the electron density at the nth harmonic becomes exponentially suppressed. For much higher s, the lifetime of the current sheets (and, respectively, the power emitted in the second wiggler) decreases. A more careful choice of s requires numerical simulations.

Many quantities may be better expressed in terms of this new parameter. For example, the length of the first wiggler [see Eq. (7)] may be rewritten as

$$N_{w1} \sim \frac{1}{4n\sigma s}, \tag{12}$$

where N_{w1} is the number of periods in the first wiggler. The initial condition Eq. (6) may also be rewritten as

$$\dot{\Phi}(\tau=0) = -\frac{2}{ns}\,\hat{u}_0, \tag{13}$$

where $\hat{u}_0 \equiv u_0/2\sigma$ is now a random variable distributed with unit standard deviation. The influence of the initial energy spread is clearly seen to decrease as s increases.

From Eqs. (5) and (6) the typical final energy spread after the first wiggler is seen to be of the order of

$$\Delta\epsilon \sim \left(\frac{a_s a_{w1}\langle \epsilon^2 \rangle}{1+a_{w1}^2}\right)^{1/2} \sim sn\sigma\epsilon. \tag{14}$$

One can see from Eq. (14) that the final energy spread is considerably larger than the initial one:

$$\frac{\Delta\epsilon}{\sigma\epsilon} \sim sn \gg 1, \tag{15}$$

as an inevitable consequence of phase area conservation. This is a crucial relation preventing further usage of the electron bunch for amplification of the radiation produced in the second wiggler.

III. X-RAY GENERATION

We now turn to the second part of the scheme, the emitter. As soon as electrons leave the first wiggler, the ponderomotive force vanishes. The process of inertial bunching, however, continues to develop, due to the redistribution of the longitudinal velocity induced by the buncher. If the length of the first wiggler and the gap between the buncher and the emitter are chosen correctly (see Sec. IV), the maximum density compression will take place inside the second wiggler. The latter one is assumed to be a wiggler with a variable magnetic-field strength, because the buncher imposes a strict condition on the beam energy [see Eq. (8)]; therefore, the only way to tune the output photon frequency is by changing the second wiggler parameter a_{w2}. As a possible solution, we consider here a planar wiggler with a variable gap between two arrays of permanent magnets; fast tuning is easily achieved with such a design [6]. Of course, there are other options: for example, a short-period electromagnetic helical wiggler would also be a good solution.

As we have shown, the first wiggler can considerably redistribute electrons within one seed-laser wavelength. The parameters of a particle trajectory at the exit of the first wiggler serve as input parameters for a description of the process of coherent spontaneous emission in the second wiggler. Particle motion in the second wiggler is assumed to be completely determined by the wiggler field, no back influence of the emitted electromagnetic waves on the emitting particles is taken into account. This approximation is justified by the fact that the seed-laser wave is out of resonance in the second wiggler, and the high-harmonic wave has too low an intensity to influence electron motion in the presence of the

large energy spread imposed by the buncher.

The energy emitted by a moving charged particle per unit solid angle per unit frequency interval is given by the textbook expression [7]

$$\frac{dE_\gamma}{d\Omega d\omega}=\frac{e^2\omega^2}{(2\pi)^2}\left|\int_{T_1}^{T_2}dt\,\vec{n}\times\vec{v}(t)e^{i\omega[t-\vec{n}\cdot\vec{r}(t)]}\right|^2, \quad (16)$$

where $\vec{n}$ is an unit vector directed along the photon momentum, and $\vec{r}(t)$ and $\vec{v}(t)$ are the particle coordinate and velocity, respectively, as functions of time t. If one is interested in the coherent radiation emitted by many particles, Eq. (16) should be modified to

$$\frac{dE_\gamma}{d\Omega d\omega}=\frac{e^2\omega^2}{(2\pi)^2}\left|\int_{T_1}^{T_2}dt\int d^3r\,d^3v\,f(\vec{r},\vec{v};t)\vec{n}\times\vec{v}e^{i\omega[t-\vec{n}\cdot\vec{r}]}\right|^2, \quad (17)$$

where $f(\vec{r},\vec{v};t)$ is the time-dependent particle distribution function.

The above expression may be simplified in our case due to the fact that all particles in the beam move in nearly the same direction and at nearly the same velocity. One may then neglect transverse motion and write the distribution function as

$$f(\vec{r},\vec{v};t)\approx\frac{1}{\pi r_0^2}\,e^{-(\vec{r}_\perp/r_0)^2}\delta(\vec{v}_\perp)f_l(z,v_z;t), \quad (18)$$

where a Gaussian beam profile (with r_0 for the waist radius) is assumed in the transverse direction and $f_l(z,v_z;t)$ describes the longitudinal evolution of the beam. As we are interested in the radiation at the fundamental frequency of the second wiggler, the above expressions may be further simplified if one neglects longitudinal velocity oscillations imposed by the wiggler field (in the case of a planar wiggler). It is convenient to separate the motion of the beam as a whole and the slow evolution of the current density inside the beam by introduction of new variables $\xi\equiv z-\langle v_z\rangle t$ and $V_\parallel\equiv v_z-\langle v_z\rangle$, where $\langle v_z\rangle$ is

$$\langle v_z\rangle\approx 1-\frac{m^2(1+a_{w2}^2/2)}{2\langle\epsilon^2\rangle}. \quad (19)$$

The longitudinal distribution function then becomes

$$f_l(z,v_z;t)=f_0(\xi-V_\parallel t,V_\parallel), \quad (20)$$

where $f_0(\xi,V_\parallel)$ is the particle distribution over the longitudinal coordinate and longitudinal velocity at the exit of the buncher (this point corresponds to $t=0$).

One may also use the small-angle approximation for photon variables, due to the fact that an ultrarelativistic particle emits electromagnetic waves in a narrow cone around the direction of its velocity [7]. With all the above simplifications, Eq. (17) becomes

$$\frac{dE_\gamma}{d^2n_\perp d\omega}=\frac{e^2\omega^2}{(2\pi)^2}\left|\int_{T_1}^{T_2}dt\int d\xi_0 dV_\parallel f_0(\xi_0,V_\parallel)\times\frac{a_{w2}m\,\sin(\Omega_{w2}\langle v_z\rangle t)}{\langle\epsilon\rangle}\exp\left[i\,\frac{\omega t m^2(1+a_{w2}^2/2)}{2\langle\epsilon^2\rangle}+i\omega t\left(\frac{n_\perp^2}{2}-V_\parallel\right)-i\omega\xi_0-n_\perp^2\left(\frac{\omega r_0}{2}\right)^2\right]\right|^2, \quad (21)$$

where we switched to $\xi_0\equiv\xi-V_\parallel t$. The factor $\exp[-n_\perp^2(\omega r_0/2)^2]$ is seen to effectively restrict angular integration to the region of very small angles:

$$n_\perp^2<(\omega r_0/2)^{-2}. \quad (22)$$

In the following we will consider the case of a sufficiently wide electron beam:

$$\omega r_0^2\gg L_{w2}, \quad (23)$$

where L_{w2} is the length of the second wiggler. Under this condition, the factor $\exp(i\omega t n_\perp^2/2)$ may be extracted from under the integral sign because in the region allowed by Eq. (22) it is nearly constant.

The next step is to take into account that the function $f_0(\xi_0,V_\parallel)$ is periodic in ξ_0 with period λ_0. Assuming the electron bunch to consist of $M\gg 1$ identical current sheets, one has

$$\frac{dE_\gamma}{d^2n_\perp d\omega}=\frac{e^2\omega^2}{(2\pi)^2}\left|\int_{T_1}^{T_2}dt\int dV_\parallel\exp\left[i\,\frac{\omega t m^2(1+a_{w2}^2/2)}{2\langle\epsilon^2\rangle}-i\omega V_\parallel t-n_\perp^2\left(\frac{\omega r_0}{2}\right)^2\right]a_{w2}m\langle\epsilon\rangle^{-1}\sin(\Omega_{w2}\langle v_z\rangle t)\times\frac{\sin(\omega\lambda_0 M/2)}{\sin(\omega\lambda_0/2)}\int_0^{\lambda_0}d\xi_0 f_0(\xi_0,V_\parallel)e^{-i\omega\xi_0}\right|^2. \quad (24)$$

There are two sharply peaked factors in the above expression. One of them is connected with the periodic particle oscillations in the wiggler field and gives, upon integration over t, a peak at the Lorenz-shifted spatial frequency of the second wiggler, the so-called spontaneous emission line. The other one comes from interference of the waves emitted by different current sheets. This factor is multiply peaked at harmonics of the seed-frequency. One may note that the interference peaks are typically more narrow than the spontaneous emission line: say, for $n\sim 50$, $M\sim 200$ interference gives the linewidth $\delta\omega/\omega\sim(nM)^{-1}\sim 10^{-4}$ while the spontaneous emission linewidth is only $\sim N_{w2}^{-1}$, where N_{w2} is the number of periods in the second wiggler. A reasonable output power is produced only when both peaks coincide. This gives the resonance condition for the second wiggler:

$$\left(1+\frac{a_{w2}^2}{2}\right)=\frac{2\Omega_{w2}\langle v_z\rangle\langle\epsilon^2\rangle}{n\omega_0 m^2}, \quad (25)$$

where n is the number of harmonic. By proper adjustment of a_{w2}, one may thus choose between different harmonics of the seed frequency.

The radiation from the second wiggler is concentrated in a small solid angle around $\vec{n}_\perp = 0$ and in a small frequency interval around $\omega = n\omega_0$. To complete our calculations, we need to integrate the spectral-angular distribution $dE_\gamma/d^2n_\perp d\omega$ over this region. Taking into account the normalization condition for $f_0(\xi_0, V_\parallel)$,

$$\int dV_\parallel \int_0^{\lambda_0} d\xi_0 f_0(\xi_0, V_\parallel) = \frac{I\lambda_0}{e}, \tag{26}$$

one has finally the following expressions for the peak power P_γ and the peak spectral brightness $dP_\gamma/d\omega$ of the coherent spontaneous radiation at the nth harmonic of the seed-laser frequency:

$$\frac{dP_\gamma}{d\omega} = \frac{a_{w2}^2 m^2 I^2}{M\pi^2 n^2 \langle \epsilon^2 \rangle r_0^2 \omega_0} |B|^2 \frac{\sin^2[M\pi(\omega - n\omega_0)/\omega_0]}{(\omega - n\omega_0)^2}, \tag{27}$$

$$P_\gamma = \frac{a_{w2}^2 m^2 I^2}{n^2 \omega_0^2 \langle \epsilon^2 \rangle r_0^2} |B|^2, \tag{28}$$

where I is the beam current and the function B is a result of averaging over the beam particles,

$$B \equiv \left\langle \frac{e^{-in\omega_0(\xi_0 + V_\parallel T_1)}(1 - e^{-in\omega_0 V_\parallel (T_2 - T_1)})}{2iV_\parallel} \right\rangle. \tag{29}$$

Assuming symmetry under the transformation ξ_0, $V_\parallel \to -\xi_0$, $-V_\parallel$, one may reduce Eq. (29) to

$$B = \left\langle V_\parallel^{-1} \sin\left(\frac{n\omega_0 V_\parallel (T_2 - T_1)}{2} \right) \times \cos\left(n\omega_0 \xi_0 + \frac{n\omega_0 V_\parallel (T_1 + T_2)}{2} \right) \right\rangle. \tag{30}$$

Equations (27)–(30) express the parameters of radiation in terms of the particle distribution function. The only step to be done is to relate the arguments of the particle distribution function, ξ_0 and $V_\parallel$, to the output parameters of electron trajectories in the buncher. The following relationships are applicable here:

$$n\omega_0 \xi_0 = n\Phi_f, \tag{31}$$

$$V_\parallel = -\frac{ns\sigma m^2 (1 + a_{w2}^2/2)}{2\langle \epsilon^2 \rangle} \dot{\Phi}_f, \tag{32}$$

where Φ_f and $\dot{\Phi}_f$ are the parameters of a particle trajectory at the exit of the first wiggler. Results of numerical simulations will be presented in the next section.

IV. NUMERICAL RESULTS

Our ID numerical model is based on the equations of motion (5) and (13). These are solved numerically for different initial conditions, to simulate the particle distribution function after the buncher and, finally, to evaluate the radiated power. To be specific, we consider 50th harmonic generation ($n = 50$) for the seed-laser wavelength $\lambda_0 = 250$ nm. The output radiation wavelength is then 5 nm in the soft x-ray range.

TABLE I. Electron-beam, seed-laser, and output radiation parameters.

Electron-beam parameters	
Beam energy ϵ	1 GeV
Peak current I	2500 A
Relative energy spread σ	10^{-3}
Beam radius r_0	50 μm
Bunch length	50 μm
Normalized emittance ϵ_N	1π (mm)(mrad)
Seed-laser parameters	
Wavelength λ_0	250 nm
Pulse power P	200 GW
Normalized intensity a_s	2.5×10^{-3}
Waist radius $L_\perp$	200 μm
Output radiation parameters	
Harmonic number n	50
Wavelength λ	5 nm
Peak power P_γ	30 MW
Bandwidth $\delta\omega/\omega$	$\sim 10^{-4}$

As for the electron-beam parameters, we adopt those of the TESLA-FEL project [8]. The aim of this project is to demonstrate the feasibility of the SASE mechanism for production of x-ray radiation. The saturated power of about 2.8 GW is expected at 6.4 nm, while the necessary wiggler length is estimated to be about 25 m. A modern superconducting linac together with the bunch compression technique will be developed to provide an extremely powerful and ''cold'' electron beam: peak current $I = 2500$ A, particle energy $\epsilon = 1$ GeV, and relative energy spread $\sigma = 10^{-3}$. The bunch length is expected to be about 50 μm. Due to the small normalized emittance of about 1π (mm) (mrad), the beam radius r_0 may also be very small, of the order of 50 μm. The parameters used in our simulations are summarized in Table I.

Our primary goal is to study the formation and dynamics of current sheets. It is convenient to characterize the degree of modulation of the particle density with the amplitudes of its Fourier components at spatial harmonics of the seed frequency. Assuming a symmetric density distribution within one seed-laser wavelength, we define the degree of modulation at the nth harmonic as

$$b_n = \langle \cos(n\omega_0 \xi) \rangle, \tag{33}$$

where ξ is the longitudinal coordinate of a particle in the comoving frame of reference. Note that the b_n parameters, although they are not directly related to the radiated power, give a more clear physical picture of the process than the much more complicated function B [see Eqs. (29) and (30)].

As an illustration, in Fig. 2 we show b_{50} as a function of the distance z between the electron bunch and the exit of the

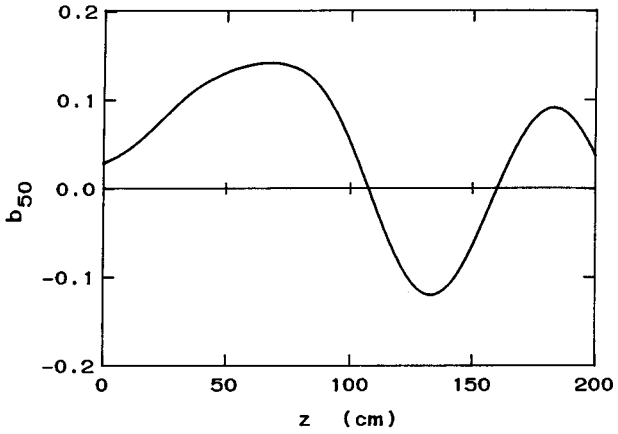

FIG. 2. Degree of beam density modulation at the 50th harmonic, b_{50}, as a function of the distance z between the electron bunch and the exit of the first wiggler. The modulation is seen to reach its maximum of 15% at about 70 cm behind the buncher. The wiggler and seed-laser parameters are $\tau=1.5$, $a_{w1}=4$, $a_{w2}=1$, $s=1$, the relative energy spread in the electron beam is 10^{-3}.

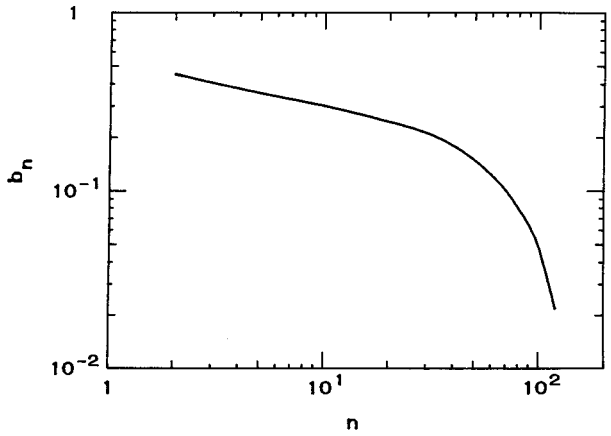

FIG. 3. Degree of modulation at the nth harmonic at the point of the peak modulation ($z=70$ cm) as a function of n. All beam and seed-laser parameters are the same as in Fig. 2.

first wiggler (note that for ultrarelativistic particles this distance is just ct). The modulation at the 50th harmonic reaches a smooth maximum at about 70 cm behind the buncher and starts to oscillate at distances exceeding 105 cm. For completeness, we varied the dimensionless length τ of the first wiggler [see Eq. (4)] in the range $1.2<\tau<1.6$. The results in Fig. 2 correspond to $\tau=1.5$; the other parameters were chosen to be $s=1$, $a_{w1}=4$, $a_{w2}=1$. The behavior seen in Fig. 2 is typical for the whole range of $1.2<\tau<1.57$; the only difference is an overall shift of the curve along the horizontal axis. As the dimensionless length of the buncher increases, the position of the peak shifts towards smaller distances; it reaches the exit of the first wiggler ($t=0$) at $\tau=\pi/2\approx1.57$. However, the peak value of the degree of modulation always remains nearly independent of τ, and rather large. This is the most surprising result: even for an initial energy spread of 10^{-3}, the density modulation at the 50th harmonic may reach 15% and remain relatively high over a distance of about 0.5 m.

The dependence of b_n on harmonic number n is shown in Fig. 3. The wiggler and the seed-laser parameters are the same as in Fig. 2; the distance from the exit of the buncher (70 cm) corresponds to the peak modulation at the 50th harmonic. A rather flat curve is observed for low harmonics while a sharp decay is seen at $n>70$. Nevertheless, even at the 100th harmonic there is still a noticeable modulation of about 5%.

Such a high degree of modulation is provided with a proper choice of the s parameter [see Eq. (11)]. Figure 4 shows the peak value of b_{50} for different values of s. The degree of modulation grows quickly at small s and tends to reach a limit of about 22% (shown as a horizontal dashed line) for $s\to\infty$. The high-s limit is a result of the anharmonicity of the ponderomotive potential well. This is the highest value reachable at the 50th harmonic with the proposed technique, even for zero energy spread in the beam. As was mentioned earlier, the results in Fig. 2 correspond to $s=1$. This value is about optimum, because it gives a high degree of modulation on the one hand, and provides a rather long lifetime of the current sheets on the other hand.

One should note that the choice of the s-parameter means actually a choice of the intensity of the seed-laser wave:

$$a_s=\frac{(n\sigma s)^2(1+a_{w1}^2)}{4a_{w1}}. \tag{34}$$

For $\sigma=10^{-3}$, $n=50$, $a_{w1}=4$, the above value of $s=1$ corresponds to $a_s\sim2.5\times10^{-3}$. In the case of a circular polarization, the power P carried by a Gaussian laser beam is

$$P=44\ \mathrm{GW}\left(\frac{a_sL_\perp}{\lambda_0}\right)^2, \tag{35}$$

where $L_\perp$ is its waist radius. One sees from Eq. (35) that focusing would reduce the required power, since the only relevant parameter in the problem is a_s. A naive approach would be to take $L_\perp$ equal to the electron beam radius ($L_\perp\sim50\ \mu$m), which would result in the seed-laser power $P\sim10$ GW. There is, however, a stronger limitation coming from the fact that the seed-laser wave intensity was assumed

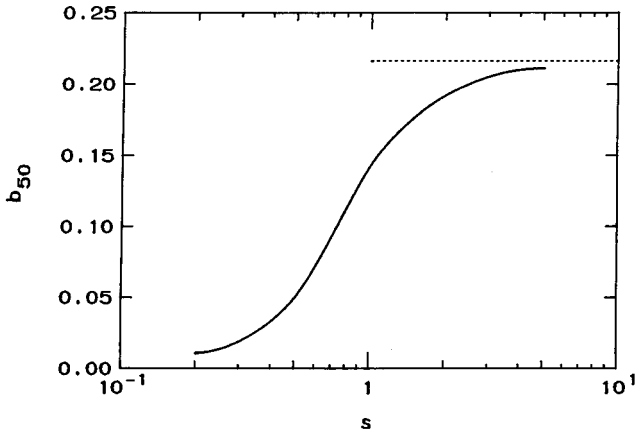

FIG. 4. Peak value of b_{50} as a function of s [see Eq. (11)]. The degree of modulation quickly increases at small s and tends to reach a limit of about 22% (shown as the horizontal dashed line) for $s\to\infty$.

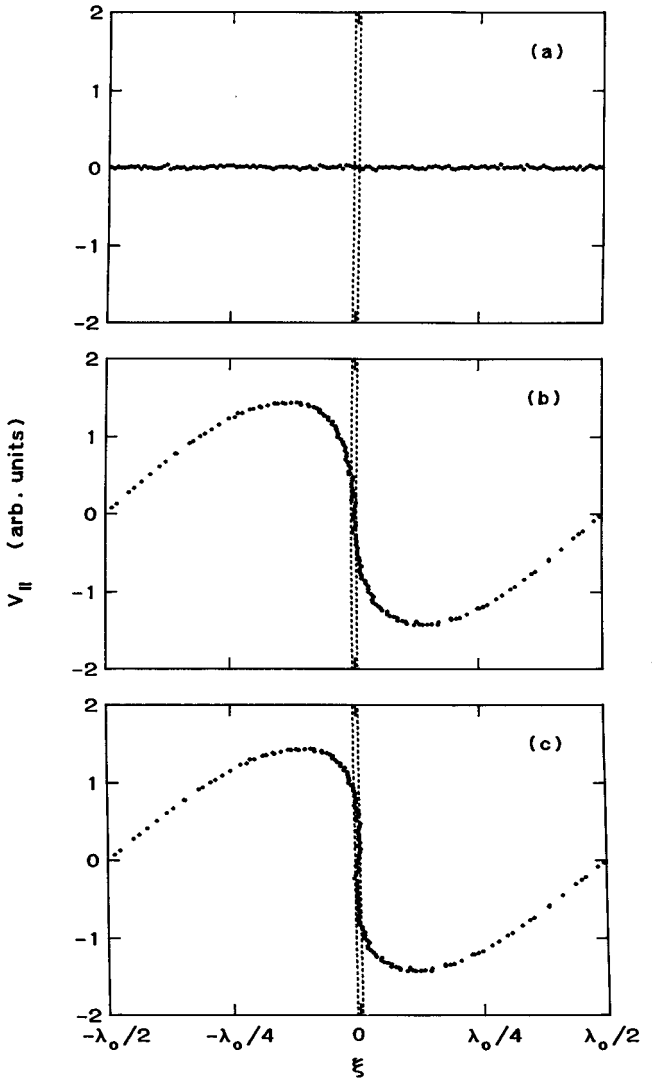

FIG. 5. Particle distribution (within one seed-laser wavelength) in the phase space defined by the longitudinal coordinate and the longitudinal velocity at three characteristic points of the system: (a) at the entrance of the buncher, (b) at the exit of the buncher, and (c) at the point of the peak modulation. All input parameters are the same as in Fig. 2. Vertical dotted lines indicate the largest interval ($=2.5$ nm) between two electrons which still enables them to coherently emit the 50th harmonic of the seed frequency.

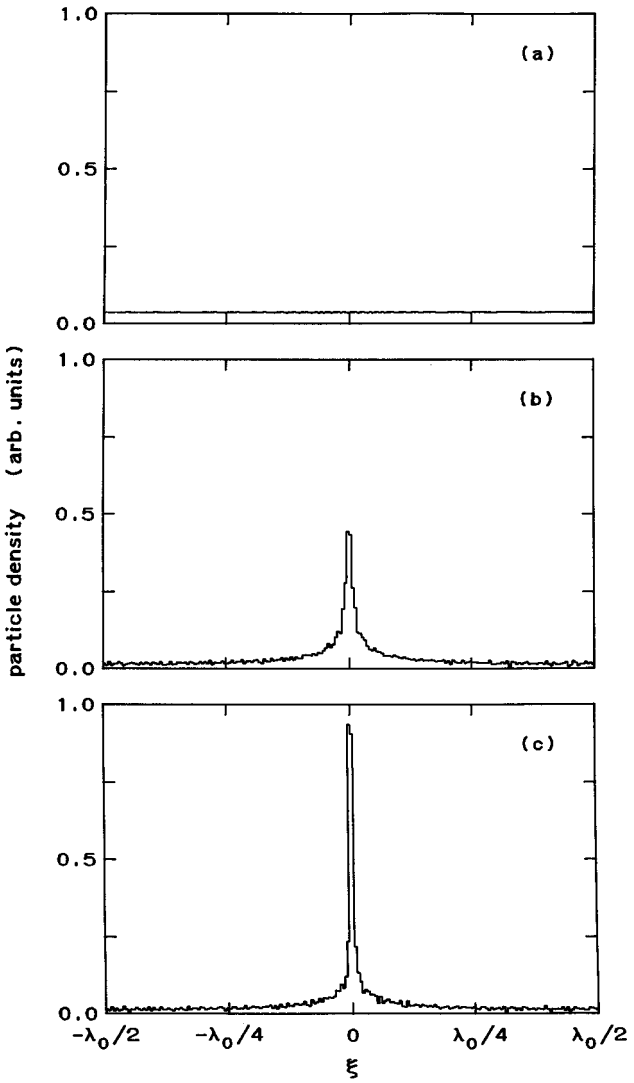

FIG. 6. Particle density profile within one seed-laser wavelength for the same three characteristic points as in Figs. 5(a)–5(c).

to be constant throughout the whole length of the first wiggler. It means that the Rayleigh length $Z_R \equiv \pi L_\perp^2/\lambda_0$ should be longer than at least half the length of the first wiggler, $Z_R > L_{w1}/2$. In combination with Eq. (35), this gives $P \sim 200$ GW, a very high but realistic power at today's technological level (see, e.g. [9,10]). A possible way to reduce the seed-laser power is to use a longer electron bunch with respectively smaller energy spread, since P depends strongly on σ: $P \sim \sigma^3$ [see Eqs. (7), (34), and (35)].

More detailed information on the formation of current sheets is given by the phase portrait of the system. In Figs. 5(a)–5(c) particle distribution (within one seed-laser wavelength) is plotted in the phase space defined by the longitudinal coordinate and the longitudinal velocity. The distribution is shown at three characteristic points of the system: at the entrance of the buncher, at the exit of the buncher, and at the point of the peak modulation. The particle density profile is shown in Figs. 6(a)–6(c) for the same three instants of time. All the input parameters are the same as in Fig. 2. Vertical dotted lines in Figs. 5(a)–5(c) indicate the thickness of a current sheet that can emit coherently at the 50th harmonic of the seed-frequency: this thickness is just $\lambda_0/100 = 2.5$ nm. One can see how the modulation builds up: the initially uniform particle distribution becomes strongly disturbed upon passage through the first wiggler, the subsequent evolution takes some time, and, finally, a significant fraction of the beam is compressed into a sheet that is a hundred times thinner than the seed-laser wavelength. At the same time, the energy spread is seen to increase dramatically, in accordance with Eq. (15).

We turn now to the photons radiated in the second wiggler. For generality, we do not assume the emitter to be situated directly behind the buncher. The time T_1 [see Eq. (30)] may be understood as a drift time, while the length of the second wiggler is given by $L_{w2} = c(T_2 - T_1)$. Quite naturally, its length as well as the gap between two wigglers must

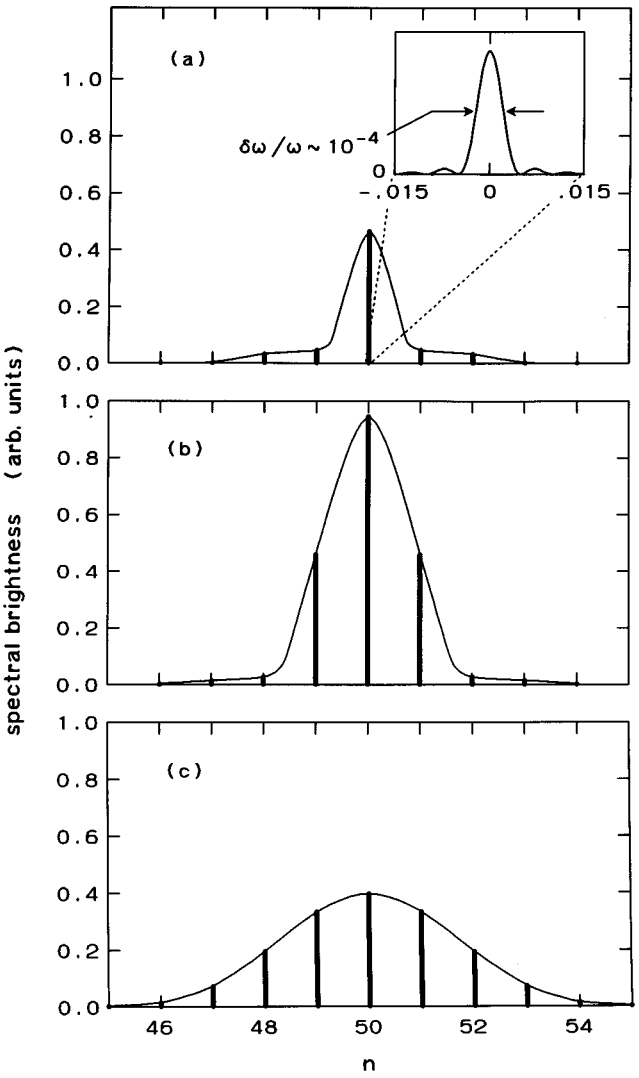

FIG. 7. Spectrum of the photons radiated in the second wiggler, for three values of the dimensionless parameter s: (a) 0.5, (b) 1, (c) 2. The inset in (a) shows the shape of a spectral line. All input parameters are the same as in Fig. 2.

be properly adjusted to cover the region of the peak modulation (see Fig. 2). However, the spectral characteristics of radiation and the output power appear to be rather insensitive to the exact values of T_1 and T_2; therefore, a good estimate may be obtained if one takes $T_1=0$ and assumes the second wiggler to occupy the whole region where b_{50} is positive.

Figures 7(a)–7(c) show the spectrum of the photons radiated from the second wiggler, for three different values of s: 0.5, 1, and 2, respectively. The emitter is assumed to be tuned at the 50th harmonic; in fact, a small number of spectral lines appears to be emitted simultaneously (solid line indicates their envelope). The relative intensities of sidebands, as well as the intensity of the central line, are seen to depend on the final energy spread imposed by the buncher [one may note that the final energy spread in the beam is nearly linear in s; see Eq. (14)]. However, the spectral width of any one harmonic is about $\delta\omega/\omega\sim10^{-4}$, independently of the energy spread. This is a characteristic feature of the seed-laser-assisted harmonic production: the perfect spatial and temporal coherence of harmonic radiation is determined

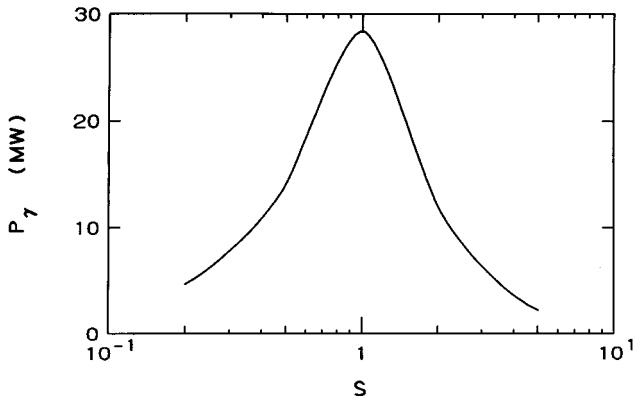

FIG. 8. Peak power radiated in the main spectral line ($n=50$), as a function of s. An optimum is seen to be reached at about $s\sim1$.

by the seed-laser wave, not by the electron-beam parameters. The inset in Fig. 7(a) illustrates the shape of a spectral line. A fine structure of the line seen as a number of small peaks on both sides of the central peak, is a result of our simplifying assumption that the bunch consists of identical current sheets; it will be smoothed out if a more realistic current profile is considered.

The peak power radiated in the main spectral line ($n=50$) is shown in Fig. 8 as a function of s. One can see that indeed there is an optimum at about $s\sim1$. With the beam parameters from Table I, the radiated power at 5 nm is then about 30 MW in a bandwidth of about 10^{-4}. The above value has to be compared to the saturated power of about 2.8 GW in a bandwidth of about 10^{-2} that is expected to be reached with 25-m-long TESLA FEL in the SASE regime [8]. Our scheme is seen to provide much lower (about two orders of magnitude) output power, while the spectral brightness is of the same order of magnitude. One should, however, take numerical estimates for both cases as very preliminary ones since no experimental evidence is available in this wavelength region. Among possible advantages of the seed-laser-based scheme are its higher stability and much better spatial coherence and smaller linewidth, since these parameters are defined by the seed laser. Last but not least, the whole length of the system appears to be about 1.6 m, over an order of magnitude shorter than in the SASE scheme.

As was already mentioned, the process of premodulation imposes a large energy spread in the electron beam; therefore, further amplification of the produced x-ray radiation is impossible with the same electron bunch. However, as a possible improvement of our scheme, one more wiggler and a ''fresh'' electron bunch (that has never been illuminated with the seed laser) from the accelerator may be used to amplify the radiation generated in the second wiggler, up to saturation. It is worth mentioning that the saturated power in the high-gain regime does not depend on the initial laser wave power but on the electron-beam parameters; therefore, one may finally reach the same power of about 2.8 GW as in the SASE case. The length of the additional amplifying section is then just about 3–4 m, as the power gain length is expected to be about 1 m [8].

To complete this section, we discuss the conditions that justify usage of the 1D approximation. Several inequalities

are to be satisfied for the 1D approximation to be valid. First of all, the initial angular spread in the electron beam is neglected. This is correct if the normalized emittance ϵ_N is sufficiently small. For our parameters, it means [see Eq. (9)]

$$\epsilon_N \ll 6\pi \ \text{(mm) (mrad)} \tag{36}$$

(note that we have assumed $\epsilon_N \sim 1\pi$ (mm) (mrad) in our numerical simulations). Second, Eq. (23) provides the condition for negligibly small influence of light diffraction on the output photon emission. For our parameters, this condition is satisfied if

$$L_{w2} \ll 2.5 \ \text{m}. \tag{37}$$

Third, the seed-laser power density is assumed to be constant over the cross section of the electron beam. This is valid under the condition

$$L_\perp \gg r_0 \sim 50 \ \mu\text{m}. \tag{38}$$

And finally, we neglected diffraction of the seed-laser wave. This is justified if

$$L_{w1} \ll \omega_0 L_\perp^2. \tag{39}$$

One may see from our numerical results that the first three conditions (36)–(38) are satisfactorily met. The condition (39) was actually used to estimate the seed-laser power; it is therefore just marginally satisfied. Hence, the most important 3D effects seem to be those related to the seed-laser pulse evolution.

V. CONCLUSIONS

We have considered the possibility to premodulate an ultrarelativistic electron beam on the nanometer length scale, so that it can produce coherent spontaneous radiation in the x-ray range. The scheme that uses the same basic elements as the high-gain harmonic generation scheme, two wigglers and a conventional seed laser, has been shown to suit this task. The first wiggler and the seed laser provide a premodulation of the beam, while the second wiggler serves as a source of radiation at a harmonic of the seed frequency. The possibility to reach ultrahigh harmonics (up to 100) is provided by the fact that, in contrast to the HGHG technique, our scheme operates at zero net gain of the seed-laser signal. The output radiation appears to be tunable between discrete harmonics of the seed frequency.

To get insight into the efficiency of premodulation, 1D numerical simulations have been performed in the one-particle approximation. For the same beam quality as in the self-amplified spontaneous emission scheme and with realistic seed-laser parameters (a wavelength of about 250 nm and a peak power of about 200 GW), the degree of beam premodulation at the 50th harmonic (5 nm) was shown to be as high as 15%. The total length of the periodic magnetic structure was shown to be of the order of several meters, an order of magnitude shorter than in the SASE case.

ACKNOWLEDGMENTS

The authors are thankful to Dr. M. Yurkov (Dubna) and Dr. E. Saldin (Samara) for helpful discussions, and to Professor J. Rossbach (DESY) for pointing out the importance of collective effects for us. This work is part of the research program of the Stichting voor Fundamenteel Onderzoek der Materie (Foundation for Fundamental Research of Matter) and was made possible by the financial support from the Nederlandse Organisatie voor Wetenschappelijk Onderzoek (Netherlands Organization for the Advancement of Research).

[1] R. Bonifacio, C. Pellegrini, and L. M. Narducci, Opt. Commun. **50**, 373 (1984).
[2] H. Winick, K. Bane, R. Boyce, J. Cobb, G. Loew, P. Morton, H.-D. Nuhn, J. Paterson, P. Pianetta, T. Raubenheimer, J. Seeman, R. Tatchyn, V. Vylet, C. Pellegrini, J. Rosenzweig, G. Travish, D. Prosnitz, E. T. Scharlemann, K. Halbach, K.-J. Kim, R. Schlueter, M. Xie, R. Bonifacio, L. De Salvo, and P. Pierini, Nucl. Instrum. Methods A **347**, 199 (1994).
[3] R. Bonifacio, L. De Salva Souza, P. Pierini, and E. T. Scharlemann, Nucl. Instrum. Methods A **296**, 787 (1990).
[4] I. Ben-Zvi, A. Friedman, C. M. Mung, G. Ingold, S. Krinsky, K. M. Yang, L. H. Yu, I. Lehrman, and D. Weissenburger, Nucl. Instrum. Methods A **318**, 208 (1992).
[5] C. A. Brau, *Free-Electron Lasers* (Academic, New York, 1990).
[6] R. J. Bakker, C. A. J. van der Geer, D. A. Jaroszynski, A. F. G. van der Meer, D. Oepts, and P. W. van Amersfoort, J. Appl. Phys. **74**, 1501 (1993).
[7] J. D. Jackson, *Classical Electrodynamics* (Wiley, New York, 1975), Chap. 14.
[8] J. Rossbach, Phys. Blätter **51**, 283 (1995).
[9] G. Mourou and D. Umstadter, Phys. Fluids B **4**, 2315 (1992).
[10] M. H. Key, Phys. Blätter **51**, 671 (1995).